Formation of Wigner molecules in small quantum dots

S. M. Reimann, M. Koskinen, and M. Manninen
Department of Physics, University of Jyväskylä, FIN-40351 Jyväskylä, Finland
(Received 29 February 2000)

It was recently argued that in small quantum dots the electrons could crystallize at much higher densities than in the infinite two-dimensional electron gas. We compare predictions that the onset of spin polarization and the formation of Wigner molecules occur at a density parameter $r_s \approx 4a_B^*$ to the results of a straightforward diagonalization of the Hamiltonian matrix.

I. INTRODUCTION

If the number of electrons artificially confined on a quasi-two-dimensional electron island (made, for example, in a semiconductor heterostructure) is very large, many properties of such a so-called quantum dot or artificial atom[1] can be described from what is known about the limit of the infinite (two-dimensional) electron gas (2DEG). Until now, most experiments[2] were performed at electron densities that are slightly below the equilibrium density of the 2DEG. The liquidlike properties then still dominate. For only a few trapped particles (as experimentally realized in vertical quantum dots[3]), pronounced addition energy maxima as a consequence of shell structure and aligned spins in the mid-shell regions due to Hund's rules were observed, in close analogy to atomic physics.[3] Even the simplest picture of N noninteracting particles in a two-dimensional harmonic trap could explain many features of the conductance spectra. For larger systems, mean field approaches like Hartree-Fock[4,5] or density functional methods[6–12] have been applied. In the small-N limit, much theoretical work has focused on exact diagonalization techniques.[13,14] This approach was mostly used for dots in magnetic fields, where correlations become increasingly important with increasing field strength. It was particularly successful in the (integer and fractional) quantum Hall regime where one can restrict the basis set to the lowest spin-polarized Landau level.[15,16] Quantum Monte Carlo[17–20] methods provide alternative approaches yielding energies whose accuracy reaches that of exact diagonalization.

When the electron density is lowered and the Coulomb energy increases relative to the kinetic energy, correlations begin to strongly dominate the electronic structure in the absence of magnetic fields also. For densities smaller than a certain critical value, a Wigner crystal[21] will be formed, in which the Coulomb interaction distributes the single electrons classically on a lattice. For the homogeneous two-dimensional electron gas, such crystallization is expected at very low densities. Monte Carlo calculations indicate that in the 2D bulk a transition to a Wigner-crystal-like state, preceded by a transition to a polarized phase,[22] occurs only at densities corresponding to Wigner-Seitz radii[23] $r_{s,2D} > 37\, a_B^*$ [the density n_0 and $r_{s,2D}$ are related by $n_0 = 1/(\pi r_{s,2D}^2)$], whereas in 3D the classical limit lies as high as $r_{s,3D} = 100 a_B^*$.[24] (In the following, for simplicity we write $r_{s,2D} = r_s$.) Chui and Tanatar[25] found that in 2D systems without translational invariance the critical density parameter for a fluid-solid transition is shifted to a considerably smaller value ($r_s \approx 7.5 a_B^*$). Could this be important for *finite* systems such as the above mentioned lateral or vertical semiconductor quantum dot structures? This question was recently posed[5,18,26] and it was argued that in finite systems confining only a few particles localization would indeed occur at significantly higher densities than in the 2D bulk. In the Wigner limit the few electrons in the trap would distribute such that their electrostatic repulsion is minimized. The internal structure of the wave function of the many-body system should then have the symmetry of the corresponding classical charge distribution. The formation of Wigner molecules, the finite-size counterpart of Wigner crystals, was found to be particularly pronounced in quantum dots with steep walls and polygonal geometry.[26] Egger *et al.*[18] have performed quantum Monte Carlo studies using a multilevel blocking algorithm.[27] For parabolic quantum dots with azimuthal symmetry they reported that at a critical density of $r_s = 4a_B^*$ the formation of Wigner-molecule-like ground states should become energetically favorable. Hartree-Fock (HF) calculations performed in an unrestricted scheme showed spin polarization, spontaneous symmetry breaking, and localization in the spatial distribution of the electronic densities of quantum dots and lateral quantum dot molecules at $r_s \approx 3.5 a_B^*$, which were attributed to the onset of Wigner crystallization.[5]

In the present article we report numerically exact configuration interaction calculations. This method has a long history in quantum chemistry, and has been applied to quantum dots by many authors.[14] Much of the previous work, however, concentrated on the electronic structure in large magnetic fields where the electron gas is polarized. Our purpose here is a comparison of the exact diagonalization results to the above mentioned recent predictions of localized states in the low-density limit and zero magnetic field. We first give a brief outline of the configuration interaction method and then turn to a discussion of the many-body spectra of a six-electron quantum dot at zero angular momentum as a function of the average electron density in the dot. Calculations for different r_s values indicate that the ground state remains unpolarized. At values of r_s that are accessible to exact diagonalization techniques, for a dot confining six electrons clear signals of formation of a Wigner molecule could not be observed. We conclude with a brief comparison to results of

density functional theory (DFT) in the local spin density approximation (LSDA) describing the electronic ground state structures.

II. METHOD AND CONVERGENCE

Consider N interacting electrons trapped in a circularly symmetric harmonic well $V(r)=m^*\omega_0^2 r^2/2$, where $r^2=x^2+y^2$. (In the quasi-two-dimensional limit one assumes that the confinement in the z direction is much stronger than in the x-y plane. Thus only the lowest subband in the z direction is populated.) We write for the Hamiltonian

$$H=\sum_{i=1}^{N}\left(\frac{-\hbar^2}{2m^*}\nabla_i^2+V(r_i)\right)+\sum_{i<j}^{N}\frac{e^2}{4\pi\varepsilon_0\varepsilon}\frac{1}{|\mathbf{r}_i-\mathbf{r}_j|}. \quad (1)$$

Here, m^* and ε are the effective mass and the dielectric constant. The calculations are done for different values of the density parameter r_s, which determines the average particle density in the dot, $n_0=1/(\pi r_s^2)$. The latter is approximated by setting the oscillator parameter $\omega_0^2=e^2/(4\pi\varepsilon_0\varepsilon m r_s^3\sqrt{N})$.[7] Throughout this paper we use effective atomic units in which the length unit a_B^* is a factor ε/m^* times the Bohr radius a_B, and the energy is given in effective hartrees, Ha$^*=(m^*/\varepsilon^2)\times 1$ hartree. (For GaAs, for example, $m^*=0.067m_e$ and $\varepsilon=12.4$, for which the length and energy units then scale to $a_B^*=97.9$ Å and Ha$^*=11.9$ meV.) To diagonalize the Hamiltonian, Eq. (1), the spatial single-particle states of the Fock space are chosen to be eigenstates of the two-dimensional harmonic oscillator with optimized oscillator parameter ω. In general, the electron-electron interaction tends to expand the system, and thus $\omega\neq\omega_0$. This effect becomes stronger with increasing r_s and we used the (empirical) relation $\omega=\omega_0/\sqrt{r_s}$. The two-body matrix elements of the electron-electron interaction are calculated using the addition theorem for $1/|\mathbf{r}_1-\mathbf{r}_2|$.[28] To set up the Fock states for diagonalization, we use eight lowest oscillator shells containing 36 states and sample over the full space with a fixed number of spin down and spin up electrons, $N_\downarrow+N^\uparrow=N$. From this sampling, only those Fock states with a given total orbital angular momentum and a configuration energy (corresponding to the sum of occupied single-particle energies) less than or equal to a specified cutoff energy E_c are included (see Fig. 1 below for an example). The purpose was to select only the most important Fock states from the full basis, thereby reducing the matrix dimension to a size $d\lesssim 10^5$. To obtain all the eigenstates we have to set $N_\downarrow=N_\uparrow=N/2$ for even particle numbers ($S_z=0$; all states with different total spin have this component), and analogously we would have $N_\downarrow=N_\uparrow\pm 1$ for odd numbers. Once the active Fock states are obtained, the Hamiltonian matrix is calculated. For Lanczos diagonalization we use the ARPACK library.[29] Finally, the total spin of each eigenvector is determined by calculating the expectation value of the $\hat{S}^2$ operator.

As mentioned above, setting up the Hamiltonian matrix from chosen Fock states and subsequent diagonalization only in principle yields an exact solution of the many-body problem. For reasons of numerical feasibility it is necessary to truncate the set of basis functions to be used in the diagonalization. One then has to make sure that convergence of the spectra is reached with respect to the cutoff. As the required matrix size increases rapidly with N, computational expenses severely restrict the calculations to only the smallest systems at not too large values of r_s. Thus, with increasing electron number or r_s, the results become less accurate due to the restricted number of basis states that can be included in the calculations. (The fact that the ground and excited states are closer in energy for larger particle number N imposes an additional difficulty.)

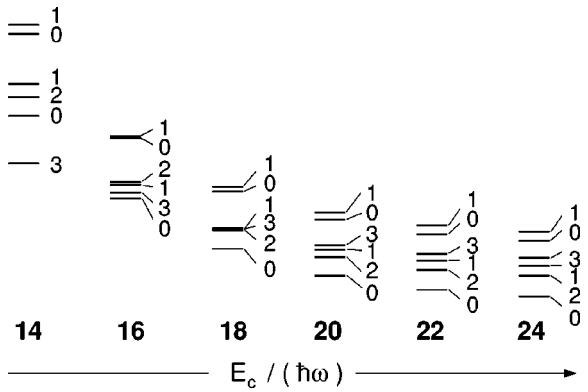

FIG. 1. Convergence of the many-body spectra of $N=6$ electrons in a harmonic trap at a density corresponding to $r_s=4a_B^*$ as a function of the cutoff energy $E_c/(\hbar\omega)$. Shown are the six lowest states with $L=0$, together with the spin S of each state.

For a quantum dot confining $N=6$ electrons at a density corresponding to $r_s=4a_B^*$ (the largest value of r_s we found accessible within the calculational scheme used here), Fig. 1 shows the convergence of the many-body spectra as a function of the cutoff energy E_c. The lowest possible Fock state for six electrons has two particles in the state $|n,l\rangle=|0,0\rangle$ and four particles in $|0,\pm 1\rangle$. Thus, the configuration energy equals $2\hbar\omega+4\times 2\hbar\omega$. This means that for the spectra with different cutoff energies displayed in Fig. 1 all excitations up to an energy $E_c-10\hbar\omega$ and belonging to the eight lowest shells[30] are included. The many-body spectra for $14\hbar\omega$ and $16\hbar\omega$ differ drastically from the results obtained for $E_c\geqslant 20\hbar\omega$. Looking at the relative ordering of the levels and the spin sequence, it becomes clear that convergence is reached only for $E_c>20\hbar\omega$. The ground state energy for zero angular momentum is $E_0=3.049$ Ha* for $22\hbar\omega$ and $E_0=3.045$ Ha* for $24\hbar\omega$. An extrapolation to infinite cutoff energy can be made by plotting the total energy as a function of $(E_c-10\hbar\omega)^{-3/2}$.[31] This gives the estimate 3.043 Ha* for the fully converged results at $r_s=4a_B^*$. For $E_c=14\hbar\omega$ a too small number of Slater determinants was included to build up the required correlations, such that the polarized $S=3$ state appeared as the ground state. (We identify a similar effect in unrestricted HF results mentioned above,[5] where the single Slater determinant that is available incorrectly favors a spin-polarized ground state.[13]) While for $E_c=22\hbar\omega$ the matrix dimension 44181 with 21 448 811 nonzero matrix elements is reasonably small, the value $E_c=24\hbar\omega$ already yields a matrix dimension 108 375 with 67 521 121 nonzero matrix elements. As for larger densities the states are less correlated, a smaller number of Slater determinants is needed for an accurate description. Density parameters larger than

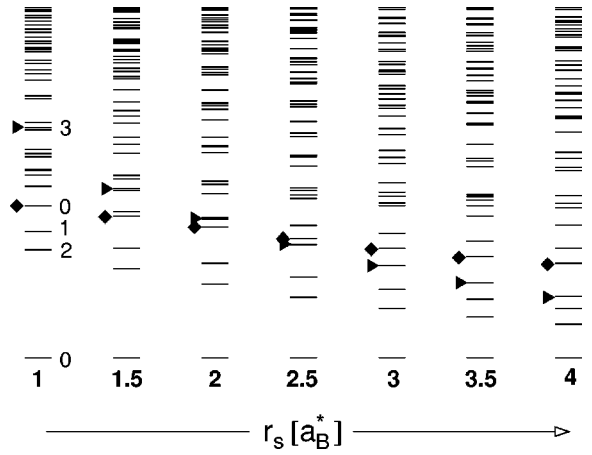

FIG. 2. Spectra for angular momentum $L=0$ and six electrons in a harmonic trap at densities corresponding to Wigner-Seitz radii between $r_s=1a_B^*$ and $r_s=4a_B^*$ in steps of $0.5a_B^*$. The square and the triangle show the first excited singlet state and the lowest fully polarized state, respectively. The lowest state always has $S=0$. The energy axis is scaled such that the energy difference between the ground state ϵ_1 and the 50th excited state ϵ_{50} equals 1, i.e., plotted are the dimensionless quantities $\tilde{\epsilon}_i=(\epsilon_i-\epsilon_1)/(\epsilon_{50}-\epsilon_1)$.

$r_s=4a_B^*$ or a higher number of particles than $N=6$ would go beyond the limits of numerical feasibility and accurate results could not be obtained.

III. MANY-BODY SPECTRA OF A SIX-ELECTRON QUANTUM DOT

We now analyze the many-body spectra and the sequence of spins for the low-lying states as the two-dimensional density parameter r_s is varied. We choose the particle number $N=6$ as it corresponds to the smallest dot size for which classically two stable crystalline structures co-exist: a pentagonal ring with one electron at the center, and a slightly distorted sixfold ring.[32,33] We fix the angular momentum to $L=0$ and show in Fig. 2 the 50 lowest states for a quantum dot confining $N=6$ particles at density parameters between $r_s=1a_B^*$ and $r_s=4a_B^*$ (in steps of $0.5a_B^*$). To obtain a better resolution of the spectra the energies of the eigenstates ϵ_i are scaled such that the energy difference between the ground state and the 50th excited state equals 1, i.e., plotted are the dimensionless quantities $\tilde{\epsilon}_i=(\epsilon_i-\epsilon_1)/(\epsilon_{50}-\epsilon_1)$. (The total energies of the ground state with $S=0$ and the excited state with $S=3$ are given in Table I below.) At a very large density corresponding to $r_s=1a_B^*$, the ground state has spin $S=0$ and is separated from the lowest excited state with spin $S=2$ by a gap of 0.49 Ha*. This state is followed by a state with $S=1$ and again another (excited) spin singlet. The lowest fully polarized state is found only at a fairly high energy, the energy difference from the $S=0$ ground state being about 0.95 Ha*. (We note that for $N=6$ at $r_s=1.73a_B^*$ we obtained excellent agreement of the $S=0$ ground state energy with the result of Pederiva *et al.*[19]) As r_s is increased, the fully polarized $S=3$ state moves down in energy. At $r_s=2.5a_B^*$ it has passed the excited singlet, but is still far from competing with the nonpolarized $S=0$ ground state. From the evolution of the energy difference between the $S=3$ state and the ground state, we do not expect any crossing of the polarized state and the ground state unless r_s becomes *much* larger than $4a_B^*$. Estimating the decrease in energy of the polarized state with respect to the ground state as r_s is increased, our data seem to support the result of Egger *et al.*[18] that the ground state of the six-electron dot is not polarized for r_s values smaller than about $8a_B^*$.

TABLE I. Energies (Ha*) for the paramagnetic ($S=0$) and ferromagnetic ($S=3$) states in a six-electron quantum dot for different densities. In the diagonalization we used $E_c=22\hbar\omega$ for $r_s\leqslant 3.5a_B^*$ and $E_c=24\hbar\omega$ for $r_s=4a_B^*$. For comparison the energies obtained with the local spin density approximation are also shown.

	Paramagnetic		Ferromagnetic	
$r_s(a_B^*)$	Exact	LSDA	Exact	LSDA
1.0	14.27	14.30	15.22	15.30
1.5	8.983	8.988	9.363	9.409
2.0	6.508	6.503	6.695	6.724
2.5	5.084	5.073	5.188	5.204
3.0	4.162	4.148	4.225	4.233
3.5	3.519	3.502	3.559	3.560
4.0	3.045	3.027	3.071	3.068

Table I compares the total energies of the ground state with spin zero and the lowest polarized state with spin $S=3$ with the corresponding result obtained from DFT, where the exchange-correlation part of the electron-electron interactions is treated in the LSDA. For the DFT results we used an interpolation formula for the Tanatar-Ceperley[23] exchange-correlation energy. We refer to Ref. 7 for further details concerning the numerical method. The configuration interaction (CI) energies of the $S=0$ ground states and $S=3$ isomer compare well with the LSDA results. For the paramagnetic case, the LSDA gives lower energies than the exact results, when $r_s\geqslant 2a_B^*$. This might be mainly due to the fact that the Tanatar-Ceperley interpolation formula slightly overestimates the correlation energy. Nevertheless, the LSDA gives surprisingly accurately the energy difference between the fully polarized ($S=3$) and the paramagnetic ($S=0$) state, as seen in Fig. 3. (For comparison, we also show the results for the infinite electron gas.)

Figure 2 shows that for $r_s=4a_B^*$ there are only two $L=0$ states between the ferromagnetic ($S=3$) state and the paramagnetic ($S=0$) ground state. However, if we consider all L values, there are several states within this energy range. This is shown in Table II where energies, spins, and angular momenta of all levels up to the first ferromagnetic state are given. Indeed, the lowest excited state has $L=1$ and $S=1$. It is possible that at very large r_s this partially polarized state might become the ground state instead of the fully polarized $S=3$ state.[18]

IV. CHARGE DENSITIES AND PAIR CORRELATION

For $r_s=4a_B^*$ the radial densities of the $S=0$ ground state and the third excited state of $L=0$, which is the lowest fully polarized state with spin $S=3$, are shown in Fig. 4. The azimuthally symmetric charge density for the polarized case shows a clear maximum at the center surrounded by an outer

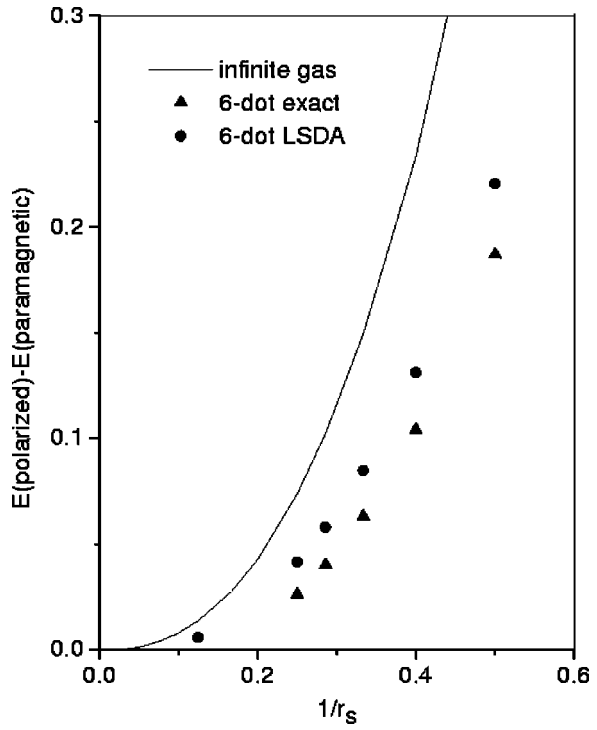

FIG. 3. Energy between the fully polarized ($S=3$) and paramagnetic states ($S=0$) for six electrons as a function of $1/r_s$. The result for the infinite 2D gas (per six electrons) is calculated using the interpolation formula of Tanatar and Ceperley (Ref. 23).

ring of lower density. In the paramagnetic case, the density profile is smoother, the maximum density being at about $r \approx 6a_B^*$. The LSDA result shows a clear minimum at the origin, while the exact result has a larger density at the center. For comparison with the results of Egger *et al.*,[18] we also show the density $\rho(r)$ multiplied by a factor $2\pi r$ (cf. lower panel of Fig. 4). For the polarized state, the maximum at the center is now seen as a clear shoulder in the density profile. Note that this is missing in the paramagnetic ground state density. (This is in disagreement with the results of Egger *et al.*[18] who found for the ground state a density profile with a clear shoulder as in the polarized case.) The azimuthal averages of the density profiles qualitatively have similarities with the broken symmetry solutions[5] of the unrestricted HF which for the paramagnetic case results in a ring of six electrons, and for the ferromagnetic case (the ground state in HF) a ring of five electrons with one electron in the center. However, the localization of the electrons is largely exaggerated in the HF calculation. In contrast, the LSDA correctly gives the paramagnetic state as the ground state, and its density profile resembles the exact result. The LSDA does not break the azimuthal symmetry until $r_s > 8a_B^*$ when spin or charge density wave like states can occur.[7] Purely classical Monte Carlo[33,32] computations have shown that for $N<6$ the charges are distributed on the perimeter of the dot, and none of the particles occupies the dot center. This changes for $N=6$, where the charge distribution with lowest energy consists of five electrons on a ring, with the remaining electron occupying the center of the dot. This configuration is labeled (5,1). If all six particles are arranged on the dot perimeter [labeled (6,0)], the classical state is stable but has a higher energy than the (5,1) configuration.

TABLE II. Energies (Ha*), spins S, and angular momenta L of all levels up to the lowest ferromagnetic state for $r_s=3a_B^*$ (left) and $r_s=4a_B^*$ (right).

$r_s=3a_B^*$			$r_s=4a_B^*$		
E(Ha*)	S	L	E(Ha*)	S	L
4.162	0	0	3.046	0	0
4.183	1	1	3.054	1	1
4.194	1	3	3.060	2	0
4.196	2	0	3.062	1	3
4.201	1	1	3.063	1	1
4.205	0	1	3.065	0	1
4.209	1	0	3.066	1	0
4.209	0	2	3.068	2	1
4.209	0	3	3.068	0	2
4.213	1	2	3.070	1	2
4.216	2	1	3.070	0	3
4.216	2	2	3.071	3	0
4.225	3	0			

The classical charge distribution can be arbitrarily oriented. The density from the CI solution, however, must be circularly symmetric. For an azimuthal average of the (5,1) pentagon structure, one would expect a pronounced maximum of the electron density in the center, and a less pronounced maximum at the dot radius. Correspondingly, the (6,0) configuration should correspond to a minimum of charge density in the center and a maximum at finite radius. A first comparison of exact diagonalization calculations with the results of the mean-field approximation was given by Pfannkuche *et al.*[13] for ''quantum dot helium,'' i.e., quantum dots containing only two electrons. They found from a comparison of exact diagonalizations with Hartree and Hartree-Fock results that the exchange and correlation contributions are crucial. While the triplet state showed a reasonable agreement between the exact and HF results, the singlet could not be well reproduced. As mentioned above, Yannouleas and Landman[5] reported that in geometrically unrestricted HF calculations at a density corresponding to $r_s \approx 3.5a_B^*$ the $N=6$ ground state is polarized and shows enhanced localization in the charge density. This $S=3$ state exhibits the same geometry as the classical distribution of six electrons in a harmonic well: five particles are equidistantly localized on the perimeter of the dot, and the sixth particle is trapped in the center of the harmonic well. The nonpolarized $S=0$ state corresponding to the (6,0) configuration is about 0.034 Ha* higher in energy. The exact diagonalization results described above do not support these HF results. Although limited to small r_s values due to the necessary restrictions of the basis set, the systematic evolution and energy sequence of CI energies and densities shown in Figs. 2 and 4 seems to indicate that polarization as well as formation of Wigner molecules in circularly symmetric, parabolic wells would be impossible at densities as large as predicted by HF calculations.[5] The geometrically unrestricted solution of the Kohn-Sham equations of Ref. 7 tends to overestimate the r_s value at which spontaneously broken spin or charge symmetries can occur in the internal structure of the wave function.[34] Although calculated in a geometrically unrestricted DFT scheme, the fully con-

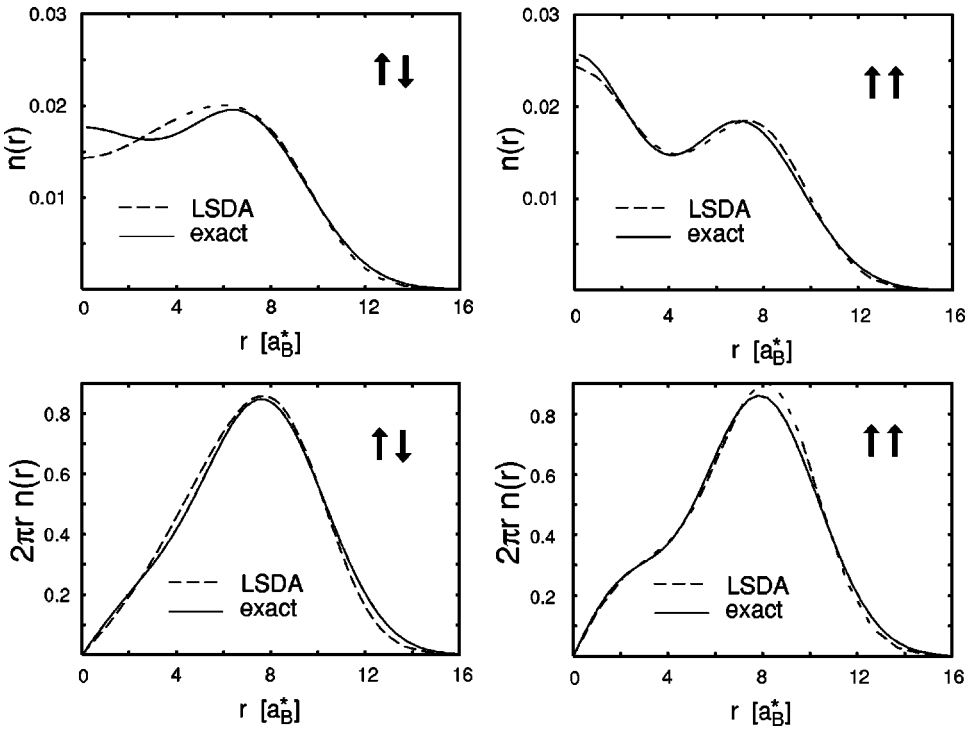

FIG. 4. Charge density of a dot confining $N=6$ electrons in a harmonic trap at $r_s=4a_B^*$; the exact result (solid line) is compared to the LSDA result (dashed line). Shown is the density $n(r)$ (upper panel) and $n(r)$ multiplied by $2\pi r$ (lower panel) for the paramagnetic $S=0$ state (left, $\uparrow\downarrow$) and the ferromagnetic $S=3$ state (right, $\uparrow\uparrow$). The $S=3$ state is separated from the $S=0$ ground state by 0.026 Ha*.

verged LSDA densities for $r_s \leqslant 4a_B^*$ shown in Fig. 4 are azimuthally symmetric. Although the LSDA suffers from the self-interaction problem, at the densities in question the results are in better agreement with CI studies than the unrestricted HF results.

It is finally of interest to study how the spin and spatial symmetry in the internal structure of the wave function can be recognized in the pair correlation function

$$g_{\uparrow\sigma}(\varphi)=\langle \hat{n}_{\uparrow}(r,0)\hat{n}_{\sigma}(r,\varphi)\rangle, \tag{2}$$

which describes the probability of finding another (spin up or down) particle if a particle with spin up is placed at $(r,0)$. Here r is the radius of maximum density and φ the angle between the electrons. Figure 5 shows $g_{\uparrow\downarrow}(\varphi)$ and $g_{\uparrow\uparrow}(\varphi)$ for the ground state (lower panel) and $g_{\uparrow\uparrow}(\varphi)$ for the excited polarized state with $S=3$ (upper panel). From the φ values of the maxima in $g_{\uparrow\sigma}(\varphi)$ one clearly concludes that the $S=0$ state has sixfold symmetry with antiferromagetic spin ordering, whereas the fully polarized case shows four maxima, corresponding to a fivefold symmetry. These intrinsic symmetries are in qualitative agreement with the unrestricted HF results, although the crystallization predicted by HF does not yet occur.

V. CONCLUSIONS

We commented on the recent conjecture that Wigner molecules would form in quantum dots at rather large electron densities $r_s \gtrsim 3.5a_B^*$.[5,18] Our results are essentially exact up to $r_s \leqslant 4a_B^*$ for six confined particles. The many-body spectra, densities, and pair correlations obtained for $N=6$ clearly illustrate that the onset of formation of Wigner molecules and, in particular, polarization of the ground state should be expected at much higher r_s values than anticipated from unrestricted HF result.[5] The critical density at which such a transition occurs does, in fact, also depend strongly on geometry[26] and on the number of confined particles at fixed average electron density in the dot. For the six-electron dot at $r_s \approx 4a_B^*$ in question,[5] the ''exact'' ground state clearly prefers $S=0$ and shows antiferromagnetic order in the pair correlation. The polarized state with C_{5v} symmetry is clearly higher in energy even than the $S=1$ state, which would also be a candidate for the classical (5,1) ground state configuration.[33,32] In addition, for values below $r_s=4a_B^*$ we did not find clear signals of rotational structure in the spectra for nonzero angular momenta that would indicate a crystal-

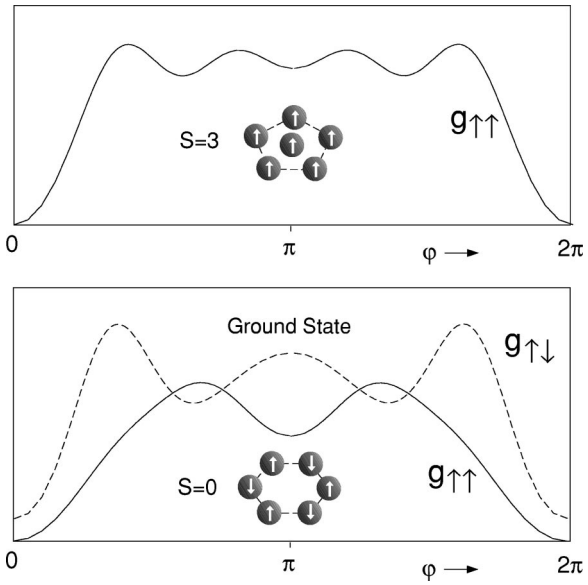

FIG. 5. Pair correlation functions $g_{\uparrow\sigma}(\varphi)$ calculated at the outer maxima of the density distribution (cf. upper panel in Fig. 4) as a function of the angle φ between the electrons for the ground state (lower panel) and the excited polarized state with $S=3$ (upper panel). The insets show schematic pictures of the electron configurations.

lized ground state. We note that the situation is different for $N<5$, where for densities as large as $r_s=2a_B^*$ the low-lying states can be well understood by assuming a square-shaped (4,0) Wigner molecule for the internal structure of the wave function and analyzing its rotational structure. This also became clear when comparing the low-energy spectrum of a Heisenberg model with four electrons on a square.[34] For $N>5$, however, this simple picture does not seem to hold, as our results for $N=6$ clearly point out. The ground state energies and densities obtained by density functional calculations in the local spin density approximation agree rather well with the results of exact diagonalization, even though this comparison was restricted to a small particle number where the accuracy of the local density approximation is questionable. This gives some confidence that the method is well suited for describing the ground state electronic structures for larger sizes.

ACKNOWLEDGMENTS

This work was supported by the Academy of Finland, the Bayerische Staatsministerium für Wissenschaft, Forschung und Kunst, and the TMR program of the European Community under Contract No. ERBFMBICT972405.

[1] R. Ashoori, Nature (London) **379**, 413 (1996).
[2] L. P. Kouwenhoven *et al.*, in *Mesoscopic Electron Tranport* of *NATO Advanced Study Institute, Series*, edited by L. L. Sohn, L. P. Kouwenhoven, and G. Schön (Plenum, New York, 1997).
[3] S. Tarucha, D. G. Austing, T. Honda, R. J. van der Hage, and L. P. Kouwenhoven, Phys. Rev. Lett. **77**, 3613 (1996).
[4] H.-M. Müller and S. E. Koonin, Phys. Rev. B **54**, 14 532 (1996).
[5] C. Yannouleas and U. Landman, Phys. Rev. Lett. **82**, 5325 (1999).
[6] M. Stopa, Phys. Rev. B **54**, 13 767 (1996).
[7] M. Koskinen, M. Manninen, and S. M. Reimann, Phys. Rev. Lett. **79**, 1817 (1997); S. M. Reimann, M. Koskinen, and M. Manninen, Phys. Rev. B **59**, 1613 (1999).
[8] O. Steffens, U. Rössler, and M. Suhrke, Europhys. Lett. **42**, 529 (1998).
[9] I.-H. Lee, V. Rao, R. M. Martin, and J.-P. Leburton, Phys. Rev. B **57**, 9035 (1998); I.-H. Lee, H.-H. Ahn, Y.-H. Kim, and R. M. Martin, *ibid.* **60**, 13 720 (1999).
[10] S. M. Reimann, M. Koskinen, M. Manninen, and B. Mottelson, Phys. Rev. Lett. **83**, 3270 (1999).
[11] D. G. Austing, S. Sasaki, S. Tarucha, S. M. Reimann, M. Koskinen, and M. Manninen, Phys. Rev. B **60**, 11 514 (1999); S. M. Reimann, J. Kolehmainen, M. Koskinen, M. Manninen, D. G. Austing, and S. Tarucha, Eur. Phys. J. D **9**, 105 (1999).
[12] K. Hirose and N. Wingreen, Phys. Rev. B **59**, 4604 (1999).
[13] D. Pfannkuche, V. Gudmundsson, and P. A. Maksym, Phys. Rev. B **47**, 2244 (1993).
[14] See, for example, P. A. Maksym and T. Chakraborty, Phys. Rev. Lett. **65**, 108 (1990); U. Merkt, J. Huser, and M. Wagner, Phys. Rev. B **43**, 7320 (1991); P. Hawrylak, Phys. Rev. Lett. **71**, 3347 (1993); A. H. McDonald and M. D. Johnson, *ibid.* **70**, 3107 (1993); S.-R. E. Yang, A. H. MacDonald, and M. D. Johnson, *ibid.* **71**, 3194 (1993); J. J. Palacios *et al.*, Phys. Rev. B **50**, 5760 (1994); P. A. Maksym, *ibid.* **53**, 10 871 (1996); T. Ezaki, N. Mori, and C. Hamaguchi, *ibid.* **56**, 6428 (1997), to mention only a few.
[15] R. B. Laughlin, Phys. Rev. B **27**, 3383 (1983).
[16] S. M. Girvin and T. Jach, Phys. Rev. B **28**, 4506 (1983).
[17] F. Bolton, Phys. Rev. B **54**, 4780 (1996).
[18] R. Egger, W. Häusler, C. H. Mak, and H. Grabert, Phys. Rev. Lett. **82**, 3320 (1999).
[19] F. Pederiva, C. J. Umrigar, and E. Lipparini, cond-mat/9912166 (unpublished).
[20] A. Harju, V. A. Sverdlov, R. M. Nieminen, and V. Halonen, Phys. Rev. B **59**, 5622 (1999).
[21] E. P. Wigner, Phys. Rev. **46**, 1002 (1934).
[22] F. Rapisarda and G. Senatore, Aust. J. Phys. **49**, 161 (1996).
[23] B. Tanatar and D. M. Ceperley, Phys. Rev. B **39**, 5005 (1989).
[24] D. M. Ceperley and B. J. Alder, Phys. Rev. Lett. **45**, 566 (1980).
[25] S. T. Chui and B. Tanatar, Phys. Rev. Lett. **74**, 458 (1995).
[26] C. E. Creffield, W. Häusler, J. H. Jefferson, and S. Sarkar, Phys. Rev. B **59**, 10 719 (1999).
[27] C. H. Mak, R. Egger, and H. Weber-Gottschick, Phys. Rev. Lett. **81**, 4533 (1998); C.H. Mak and R. Egger, J. Chem. Phys. **110**, 12 (1999).
[28] M. Weissbluth, *Atoms and Molecules* (Academic Press, New York, 1978).
[29] R. B. Lehoucq, D. C. Sørensen, and Y. Yang (unpublished); see http://www.caam.rice.edu/software/ARPACK
[30] For the highest cutoff values the limitation to eight oscillator shells leaves out configurations where one electron is excited to a high energy level, while the others stay on lower levels. In our experience, these configurations are not important for the correlation energies.
[31] M. Koskinen, M. Manninen, and P. O. Lipas, Phys. Rev. B **49**, 8418 (1994).
[32] F. Bolton and U. Rössler, Superlattices Microstruct. **13**, 139 (1992).
[33] V.M. Bedanov and F.M. Peeters, Phys. Rev. B **49**, 2667 (1994).
[34] M. Koskinen, M. Manninen, B. Mottelson, and S.M. Reimann, cond-mat/0004095 (unpublished).